NEUROSCIENCE

Differential contribution of APP metabolites to early cognitive deficits in a TgCRND8 mouse model of Alzheimer's disease

Valentine Hamm,[1,2] Céline Héraud,[1,2] Jean-Bastien Bott,[1,2] Karine Herbeaux,[1,2] Carole Strittmatter,[1,2] Chantal Mathis,[1,2] Romain Goutagny[1,2]*

Alzheimer's disease (AD) is a neurodegenerative pathology commonly characterized by a progressive and irreversible deterioration of cognitive functions, especially memory. Although the etiology of AD remains unknown, a consensus has emerged on the amyloid hypothesis, which posits that increased production of soluble amyloid β (Aβ) peptide induces neuronal network dysfunctions and cognitive deficits. However, the relative failures of Aβ-centric therapeutics suggest that the amyloid hypothesis is incomplete and/or that the treatments were given too late in the course of AD, when neuronal damages were already too extensive. Hence, it is striking to see that very few studies have extensively characterized, from anatomy to behavior, the alterations associated with pre-amyloid stages in mouse models of AD amyloid pathology. To fulfill this gap, we examined memory capacities as well as hippocampal network anatomy and dynamics in young adult pre-plaque TgCRND8 mice when hippocampal Aβ levels are still low. We showed that TgCRND8 mice present alterations in hippocampal inhibitory networks and γ oscillations at this stage. Further, these mice exhibited deficits only in a subset of hippocampal-dependent memory tasks, which are all affected at later stages. Last, using a pharmacological approach, we showed that some of these early memory deficits were Aβ-independent. Our results could partly explain the limited efficacy of Aβ-directed treatments and favor multitherapy approaches for early symptomatic treatment for AD.

INTRODUCTION

Alzheimer's disease (AD) is a neurodegenerative pathology commonly characterized by a progressive and irreversible deterioration of cognitive functions, especially memory, which accentuates with the progression of the disease. Although the etiology of AD remains unknown, a consensus has emerged on the amyloid hypothesis (*1*), which posits that the amyloid β (Aβ) peptide, a major constituent of the amyloid plaques, induces neuronal network dysfunctions and is therefore responsible for the alteration of cognitive functions (*2*). Aβ derives from the amyloidogenic cleavage of the transmembrane amyloid precursor protein (APP, also called β-amyloid precursor protein), first by the β-secretase enzyme (β-secretase or BACE-1), which generates soluble APP (sAPP) and the β–C-terminal fragment (β-CTF, also called C99). β-CTF is then cleaved by the γ-secretase enzyme (γ-secretase) to generate the Aβ peptide and the amyloid intracellular domain (AICD). Aβ, principally Aβ containing 42 amino acids ($Aβ_{42}$), aggregates to form Aβ oligomers and extracellular amyloid plaques. Over the last 15 years or so, it has become clear that neural networks and memory impairments are due to increased brain levels of soluble forms of Aβ (*3*, *4*) rather than amyloid fibrils or amyloid plaques (*5*). Thus, efforts aimed at lowering Aβ levels have been deployed as a possible treatment for AD, mainly by using γ-secretase inhibitors. However, these drugs paradoxically induced no improvement or even worsened cognitive function and/or had drastic side effects that preclude their use as suitable therapeutics for AD (*6*). The lack of obvious beneficial effects on cognition suggests that Aβ alone is unable to account for all aspects of the disease (*7*, *8*). Accordingly, other amyloid factors, such as β-CTF (*9*–*15*), AICD (*16*), or the newly described CTF-η (*17*), could represent possible culprits in early AD. Therefore, characterizing whether different APP cleavage products contribute differentially to early cognitive deficits (that is, before amyloid plaque apparition) is of utmost importance. To this aim, we performed a comprehensive characterization of 2-month-old male TgCNRD8 mice and their nontransgenic control littermates (NTg). At this age, TgCRND8 mice exhibit no plaques and low levels of Aβ associated with high expression of β-CTF within the hippocampus. We first showed that these mice present drastic alterations in CA1 inhibitory networks and γ oscillations, indicating that hippocampal networks are affected early in the time course of the amyloid pathology. Even if multiple forms of memory are affected in AD, specific functions such as recognition memory for objects, detection of spatial changes, and spatial navigation seem precociously altered (*18*–*20*). Although these forms of memory rely on complex interstructure dialogs encompassing the temporal lobe and prefrontal cortex, most of them are known to be dependent on the integrity of hippocampal networks [for a recent review on recognition memory, see the study of Ameen-Ali *et al.* (*21*)]. Therefore, the early hippocampal alterations reported in young TgCRND8 mice might be responsible for some subtle memory impairment. Accordingly, pre-plaque TgCRND8 mice exhibited a particular pattern of memory deficits: They were impaired in both spatial object location and object-place association tasks, but they performed as well as their NTg littermates in the novel object recognition task and the Barnes maze spatial navigation task. Last, because both β-CTF and Aβ were detected in the hippocampus of pre-plaque TgCRND8 mice, it was critical to assess the respective role of each APP fragment in the reported memory deficits. To target different APP cleavage products, we chronically treated TgCRND8 mice and their NTg littermates with either β- or γ-secretase inhibitors. We showed that behavioral deficits in the spatial object location task were most likely Aβ-dependent because they were rescued by both the

[1]Laboratoire de Neurosciences Cognitives et Adaptatives (LNCA), Université de Strasbourg, Faculté de Psychologie, 12 rue Goethe, F-67000 Strasbourg, France. [2]LNCA, UMR 7364, CNRS, Neuropôle de Strasbourg, 12 rue Goethe, F-67000 Strasbourg, France.
*Corresponding author. Email: goutagny@unistra.fr

β- and γ-secretase inhibitors, which precludes Aβ generation, while deficits in the object-place association task were likely Aβ-independent because they were rescued only by the β-secretase inhibitor, which prevents both Aβ and β-CTF production. Further, we showed that Aβ and β-CTF likely act on specific hippocampal networks. Overall, our study indicates differential contributions of APP amyloid metabolites to early memory deficits, highlighting the complexity of developing an effective therapeutic strategy against AD.

RESULTS

Hippocampal amyloidogenic state in young TgCRND8 mice

To characterize the hippocampal amyloid state in young pre-plaque TgCRND8 mice [before 3 months of age (*22*)], we performed Western blot analysis of a whole hippocampal extract using the APP C-term antibody (which recognizes murine as well as human mutated APP and related proteolytic products) in 1- and 2-month-old TgCRND8 and NTg littermate mice. As already described in the study of Goutagny *et al.* (*9*) and in the study of Cavanagh *et al.* (*23*), young TgCRND8 mice exhibited an age-dependent increase of CTF levels in the hippocampus [two-way analysis of variance (ANOVA): interaction age × genotype: $F_{1,22} = 4.342$, $P = 0.049$; Bonferroni post hoc between 1- and 2-month-old TgCRND8: $t_{22} = 4.262$, $P = 0.0019$; Fig. 1A]. The anti-human Aβ antibody (6E10) applied on the same samples did not detect Aβ at these ages but revealed and confirmed the increased level of human β-CTF (fig. S1). To test whether Aβ was present in hippocampal networks, we performed enzyme-linked immunosorbent assay (ELISA) analyses on a subset of these extracts; this approach allowed the detection of very small quantities of Aβ (around 0.2 ng/mg of hippocampal protein homogenates). Although Aβ was not detectable in NTg animals, low levels were present in TgCRND8 mice starting at 1 month of age, with a tendency to increase at between 1 and 2 months ($t_8 = 1.505$, $P = 0.1707$; Fig. 1B). Therefore, in addition to β-CTF, the hippocampus of young TgCRND8 mice also contains Aβ.

Hippocampal network structure and function in young TgCRND8 mice

To determine whether the amyloidogenic state described above could be linked to alterations in hippocampal activity as already described in vitro (*9*), we performed in vivo multisite electrophysiological recordings in urethane-anesthetized animals. We used 16-channel linear silicon probes to simultaneously record from different layers of the dorsal hippocampus (CA1, from stratum oriens to stratum lacunosum moleculare; Fig. 2A). Both TgCRND8 ($n = 8$) and NTg mice ($n = 11$) exhibited clear θ oscillations after sensory stimulation in all CA1 layers (Fig. 2A). We then quantified the integrated power of total, θ, slow γ (SG), and fast γ (FG) oscillations in the CA1 area. No differences were found between genotypes in both total and θ powers (two-way ANOVA for total power: genotype effect: $F_{1,17} = 0.3680$, $P = 0.5521$; two-way ANOVA for θ power: genotype effect: $F_{1,17} = 0.2852$, $P = 0.6002$; Fig. 2B). However, a slight decrease in θ frequency was observed (controls versus TgCRND8: $t_{17} = 2.195$, $P = 0.0423$). γ Oscillatory activity was largely impaired in young TgCRND8 mice in both the SG (two-way ANOVA for SG power: interaction depth × genotype: $F_{8,136} = 3.182$, $P = 0.0024$; Fig. 2B) and FG ranges (two-way ANOVA for FG power: interaction depth × genotype: $F_{8,136} = 2.299$, $P = 0.0242$; Fig. 2B).

At the cellular level, inhibitory interneurons expressing either parvalbumin (PV) or somatostatin (SOM) have been critically linked to hippocampal oscillatory activity (*24*, *25*) and have been shown to be precociously altered in mouse models of AD (*26*, *27*). Therefore, we performed immunolabeling of SOM and PV interneurons in the hippocampus of young TgCRND8 and NTg littermates (Fig. 3A). More specifically, we quantified the numbers of SOM and PV interneurons in the different subfields of the dorsal hippocampus. Although no difference was found in the number of SOM interneurons (two-way ANOVA: genotype effect: $F_{1,7} = 0.2589$, $P = 0.6265$; Fig. 3A), we could show that TgCRND8 mice exhibited a significant decrease of PV interneurons specifically in the CA1 area (two-way ANOVA: genotype effect: $F_{1,7} = 7.461$, $P = 0.0293$; hippocampal subfield effect: $F_{3,21} = 212.5$, $P < 0.0001$; Bonferroni post hoc test for CA1: $t_{28} = 3.680$, $P = 0.0039$; Fig. 3A). To confirm that the decrease in the number of immunofluorescent PV interneurons found in TgCRND8 mice resulted from a decrease in the number of cells rather than a decrease in PV expression per se, we quantified the level of voltage-gated sodium channel subunits NaV1.1 and NaV1.6, which are predominant in PV cells (*26*). These experiments demonstrated that TgCRND8 mice exhibited a significant decrease in the expression of NaV1.6 (NTg versus TgCRND8: $t_9 = 3.1$, $P = 0.0127$) and also suggested a decrease for the NaV1.1 subunit (NTg versus TgCRND8: $t_9 = 2.015$, $P = 0.0747$; Fig. 3B). Together, these results indicate that young TgCRND8 mice present profound alterations in dorsal hippocampal CA1 PV inhibitory networks, likely leading to altered γ oscillations.

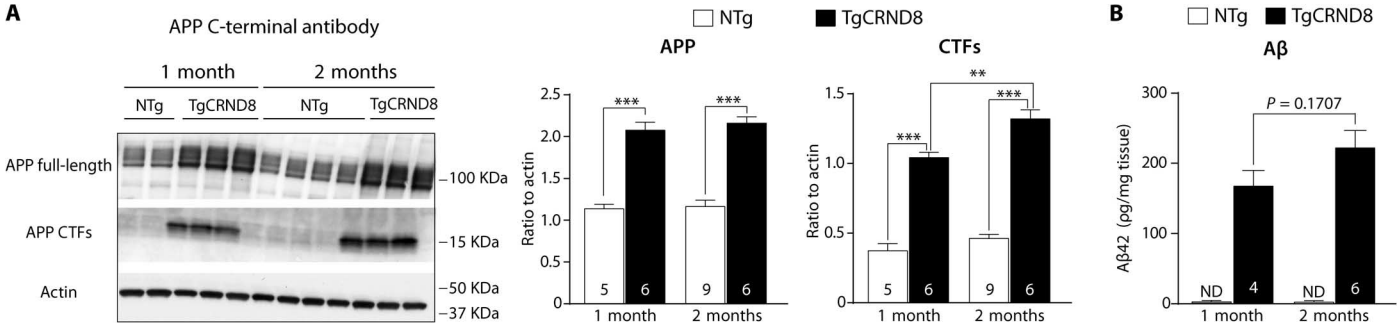

Fig. 1. Semiquantitative analyses of the expression of APP and APP metabolites in 1- and 2-month-old TgCRND8 and control littermate mice. (**A**) Western blot using the APP C-term antibody and quantification of APP and CTF levels. Note the specific increase in CTF levels in 2-month-old TgCRND8 mice compared to 1-month-old animals. (**B**) Hippocampal Aβ42 dosage in 1- and 2-month-old NTg and TgCRND8 mice. Aβ42 is below detection level in NTg animals. Despite a tendency to an age-dependent increase, Aβ levels remain low in both groups. *, difference between groups (**$P < 0.01$ and ***$P < 0.0001$); ND, non detectable.

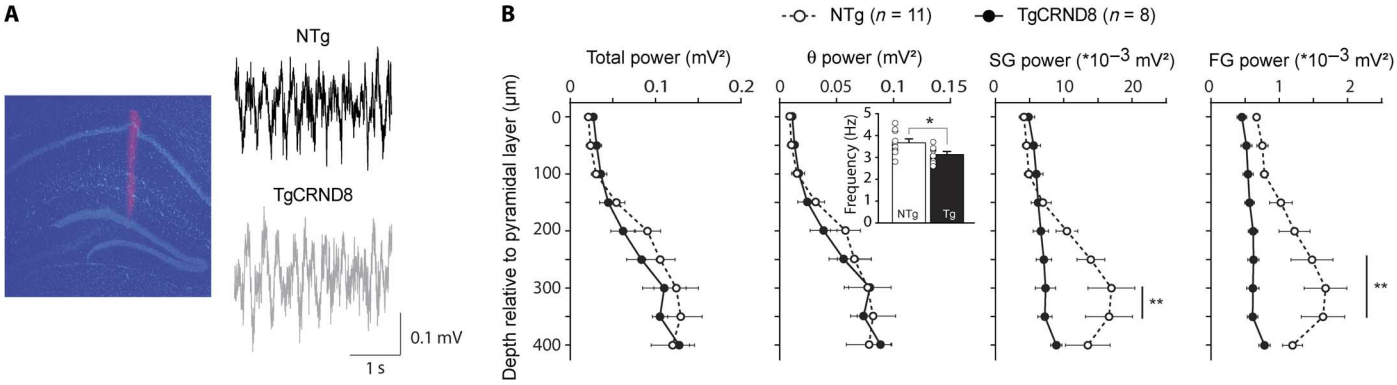

Fig. 2. Alterations in hippocampal oscillatory activity in pre-plaque TgCRND8 mice. (**A**) Both TgCRND8 and NTg mice exhibit clear θ oscillations after sensory stimulation in all CA1 subfields. (**B**) No differences were found between genotypes in both total and θ power. γ Oscillatory activity was largely impaired in pre-plaque TgCRND8 mice in both the SG and FG range. (*, difference between groups; *$P < 0.05$ and **$P < 0.01$).

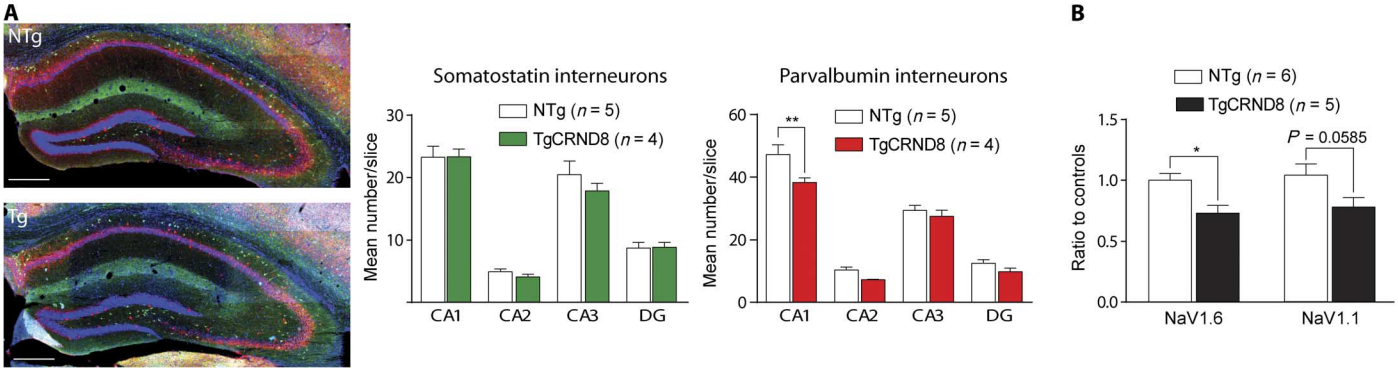

Fig. 3. Alterations in hippocampal PV inhibitory network in pre-plaque TgCRND8 mice. (**A**) Photomicrograph of the dorsal hippocampus from NTg and pre-plaque TgCRND8 mice [PV, red; SOM, green; 4′,6-diamidino-2-phenylindole (DAPI), blue]. Scale bars, 200 µm. No change was seen in the number of SOM interneurons whatever the hippocampal subfield. However, pre-plaque TgCRND8 mice exhibited a significant decrease in PV interneurons only in the CA1 area of the dorsal hippocampus. (**B**) Western blot analyses of hippocampal expression of NaV1.1 and NaV1.6 subunits. TgCRND8 mice exhibited a significant decrease in the expression of NaV1.6 and a clear tendency toward a decrease for the NaV1.1 subunit. *, difference between genotypes, Bonferroni post-hoc test, *$P < 0.05$ and **$P < 0.01$.

Behavioral performances of young TgCRND8 mice

Hippocampal oscillatory activity has been described as a critical player in memory encoding, consolidation, and retrieval. To determine whether the specific alterations found in dorsal hippocampal CA1 networks could be linked to cognitive deficits, we performed a battery of behavioral tests in young adult 2-month-old male TgCRND8 mice. We first used three tests relying on spatial information treatment by dorsal CA1 hippocampal networks: the spatial object location task (*28*, *29*), the object-place association task (*28*, *30*), and the Barnes maze task (*31*).

TgCRND8 mice were impaired in both the spatial object location task (different from chance level: NTg: $t_{13} = 2.311$, $P = 0.0379$; TgCRND8: $t_9 = 0.8115$, $P = 0.483$; group difference: NTg versus TgCRND8: $t_{22} = 1.735$, $P = 0.0968$; Fig. 4A and fig. S2) and the object-place association task (different from chance level: NTg: $t_{13} = 2.311$, $P = 0.0379$; TgCRND8: $t_9 = 0.8115$, $P = 0.483$; group difference: NTg versus TgCRND8: $t_{22} = 2.046$, $P = 0.05$; Fig. 4B and fig. S3). However, they performed as well as the control littermates in the Barnes maze task either in the learning phase or during the probe test (two-way ANOVA for learning: genotype effect: $F_{1,21} = 1.896$, $P = 0.183$; two-way ANOVA for probe: genotype effect: $F_{1,21} = 1.595$, $P = 0.2205$; Fig. 4C and fig. S4).

Mice were also tested in a short-term novel object recognition task, which is mainly considered as hippocampal-independent [see the study of Ameen-Ali *et al.* (*21*) for a recent review]. TgCRND8 mice performed as well as their respective control littermates, with a clear detection of the novel object (different from chance level: NTg: $t_{13} = 4.255$, $P = 0.0009$; TgCRND8: $t_{12} = 3.151$, $P = 0.0084$; group difference: NTg versus TgCRND8: $t_{25} = 0.8203$, $P = 0.4198$; Fig. 4D and fig. S5). Together, these results indicate that pre-plaque TgCRND8 mice exhibited early cognitive deficits only in a subset of hippocampal-dependent tasks.

Differential involvement of β-CTF and Aβ in early cognitive deficits

Because both β-CTF and Aβ were detected in the hippocampus of young TgCRND8 mice, it was critical to assess their respective role, if any, in the cognitive deficits reported above. To do so, we chronically treated NTg and TgCRND8 mice with either a β-secretase inhibitor [LY2811376, 15 mg/kg every 2 days for 1 month between 1 and 2 months; this drug decreases both β-CTF and Aβ levels without affecting the expression of APP (*32*)] or a γ-secretase inhibitor [semagacestat, 10 mg/kg per day for 8 days; this drug decreases Aβ levels but increases β-CTF

contents (*12*)]. Mice were tested at the age of 2 months in the spatial object location task followed by the object-place association task. None of the treatments had an effect on memory performance in NTg animals (one-way ANOVA for the spatial object location task: $F_{2,41} = 0.3607$, $P = 0.6993$; one-way ANOVA for the object-place association task: $F_{2,42} = 0.2040$, $P = 0.8163$; Fig. 5, A and B, and fig. S6). Both treatments were able to rescue retention performances of TgCRND8 mice in the spatial object location task (different from chance level: NTg-vehicle: $t_{23} = 6.61$, $P < 0.0001$; NTg-LY2811376: $t_6 = 6.951$, $P = 0.0004$; NTg-semagacestat: $t_{12} = 4.444$, $P = 0.0008$; TgCRND8-vehicle: $t_{21} = 0.6681$,

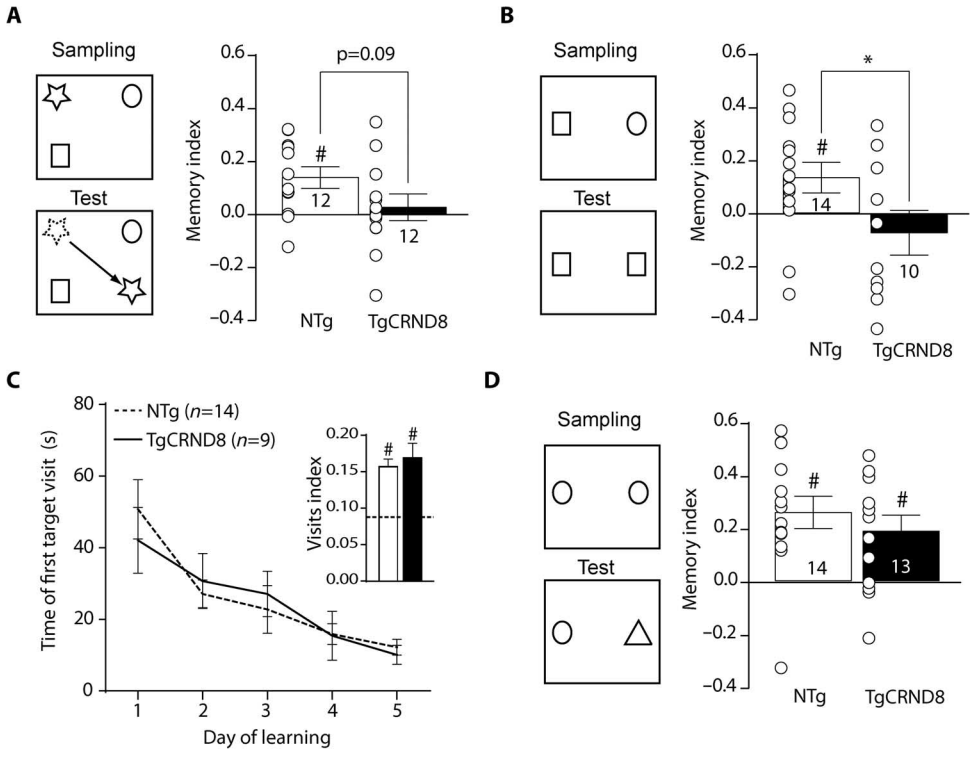

Fig. 4. Behavioral characterization of 2-month-old pre-plaque TgCRND8 mice. Pre-plaque TgCRND8 mice presented drastic alterations in the spatial object location task (**A**) and the object-place association task (**B**). However, they performed as controls in the Barnes maze task during the training phase and the probe test (**C**) as well as the novel object recognition task (**D**). *, difference between genotypes; #, different from chance.

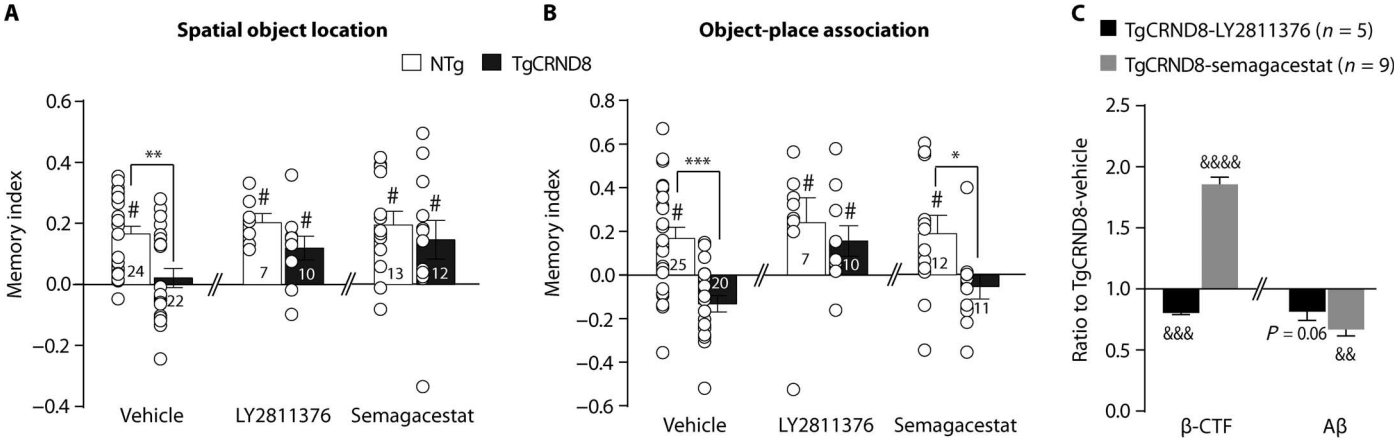

Fig. 5. Differential effect of β-secretase (LY2811376) and γ-secretase (semagacestat) inhibition on memory performances in pre-plaque TgCRND8 mice. (**A**) Both β- and γ-secretase inhibitors rescued retention performances in the spatial object location task. (**B**) However, in the object-place association task, only the β-secretase inhibitor was effective. (**C**) LY2811376 and semagacestat differentially affected APP metabolite production. Although both treatments decreased Aβ levels, LY2811376 and semagacestat have opposite effects on β-CTF levels. (*, difference between genotypes * $P < 0.05$, ** $P < 0.01$, and *** $P < 0.001$); #, difference from chance; &, difference from TgCRND8 + vehicle ($^{\&\&}P < 0.01$, $^{\&\&\&}p < 0.001$, and $^{\&\&\&\&}P < 0.0001$).

$P = 0.5113$; TgCRND8-LY2811376: $t_9 = 3.106$, $P = 0.0126$; TgCRND8-semagacestat: $t_{11} = 2.303$, $P = 0.0418$; Fig. 5A) without affecting the total exploration time during the acquisition trial (fig. S7). Two-way ANOVA revealed only a genotype effect ($F_{1,8} = 7.156$, $P = 0.009$), and the Bonferroni post hoc analysis showed that TgCRND8 mice exhibited a decrease in retention performances compared to NTg littermates only in the vehicle-treated group ($t_{82} = 3.3$, $P = 0.0043$). Surprisingly, only the LY2811376 treatment was able to rescue memory performances in the object-place association task, with no effect of the semagacestat treatment (different from chance level: NTg-vehicle: $t_{24} = 3.259$, $P = 0.0033$; NTg-LY2811376: $t_6 = 7.405$, $P = 0.0003$; NTg-semagacestat: $t_{11} = 2.264$, $P = 0.0448$; TgCRND8-vehicle: $t_{19} = 3.523$, $P = 0.0023$; TgCRND8-LY2811376: $t_9 = 2.230$, $P = 0.05$; TgCRND8-semagacestat: $t_{10} = 0.9314$, $P = 0.3736$; Fig. 5B). Neither the LY2811376 treatment nor the semagacestat treatment affected total object exploration during the acquisition trial (fig. S8). Two-way ANOVA revealed a genotype effect ($F_{1,80} = 13.98$, $P = 0.0003$) and a treatment effect ($F_{2,80} = 3.594$, $P = 0.032$) without interaction ($F_{2,80} = 1,299$, $P = 0.2786$). Bonferroni post hoc analysis revealed that TgCRND8 mice exhibited a decrease in retention performances as compared to NTg littermates in both the vehicle-treated group ($t_{80} = 4.176$, $P = 0.0002$) and the semagacestat-treated group ($t_{80} = 2.429$, $P = 0.05$) but not in the LY2811376-treated group ($t_{80} = 0.7348$, $P > 0.999$). To confirm the effect of both treatments on hippocampal APP metabolite expression, we quantified the levels of Aβ using ELISA and those of β-CTF using Western blot analysis (Fig. 5C). As already shown in the study of Mitani *et al.* (*12*) and the study of May *et al.* (*32*), we found that hippocampal Aβ concentration was reduced following both treatments (one-sample *t* test against TgCRND8-vehicle: TgCRND8-LY2811376: $t_4 = 2.536$, $P = 0.0642$; TgCRND8-semagacestat: $t_8 = 4.346$, $P = 0.0026$). In addition, we also confirmed that hippocampal β-CTF contents were decreased following the LY2811376 treatment but increased after the semagacestat treatment (one-sample *t* test against TgCRND8-vehicle: TgCRND8-LY2811376: $t_4 = 14.42$, $P = 0.0001$; TgCRND8-semagacestat: $t_8 = 14.30$, $P < 0.0001$). Given the distinct effect of LY2811376 and semagacestat treatments on both APP metabolite levels and cognitive performances, it is likely that different APP metabolites are responsible for the deficits of TgCRND8 mice in the spatial object location task and in the object-place association task.

Differential effect of β- and γ-secretase on dorsal hippocampal network functioning

Because TgCRND8 mice exhibit specific alterations in CA1 PV networks, we wondered whether LY2811376 and/or semagacestat treatments might act via a rescue of CA1 interneuronal networks. To this aim, we performed immunolabeling of PV interneurons in a subset of NTg and TgCRND8 mice following vehicle or pharmacological treatment (vehicle: $n = 7$ NTg and 8 TgCRND8; LY2811376: $n = 3$ TgCRND8; semagacestat: $n = 6$ TgCRND8). None of the treatments were able to rescue the PV interneuron network in TgCRND8 mice (one-way ANOVA: $F_{3,20} = 6.56$, $P = 0.0029$; Fig. 6). The number of PV^+ neurons was still significantly decreased following semagacestat (Bonferroni post hoc test: $t_{20} = 3.807$, $P = 0.0066$) or LY2811376 treatment (Bonferroni post hoc test: $t_{20} = 3.467$, $P = 0.00146$; Fig. 6). In addition to a decrease in PV^+ cells, young TgCRND8 mice exhibit a decrease in NaV expression. Because restoring NaV levels in a mouse model of AD restores memory deficits (*26*), we tested whether LY2811376 and/or semagacestat might rescue NaV1.1 and/or NaV1.6 levels in the hippocampus. We showed that semagacestat was able to rescue levels of both NaV1.1 and NaV1.6, while LY2811376 only rescued those of NaV1.6 (one-way ANOVA for NaV1.1: $F_{3,23} = 6.52$, $P = 0.0024$; one-way ANOVA for NaV1.6: $F_{3,23} = 5.911$, $P = 0.0038$; Fig. 6). Therefore, beneficial effects of β- and γ-secretase inhibitor treatments on the spatial object location task might be mediated, in part, by a rescue of the NaV levels, thereby restoring "normal" PV interneuron function (*26*).

We then questioned how LY2811376 might rescue memory performances in the object-place association task. Semagacestat appears more powerful than LY2811376 in rescuing PV interneuron function in CA1, but it has no effect on the object-place deficit. Thus, another region could have mediated the beneficial effect of LY2811376 in the object-place task. Because some studies indicate that upstream regions of CA1 might be involved (*33*), we performed c-Fos immunolabeling of activated cells in the dorsal hippocampus following the object-place association task in NTg and TgCRND8 mice. We found that the dentate gyrus was the most activated hippocampal area during the task (two-way ANOVA: hippocampal subregion effect: $F_{2,24} = 51.53$, $P < 0.001$; Fig. 7A). Strikingly, dentate activation during the task was markedly reduced in TgCRND8 mice (interaction genotype ×

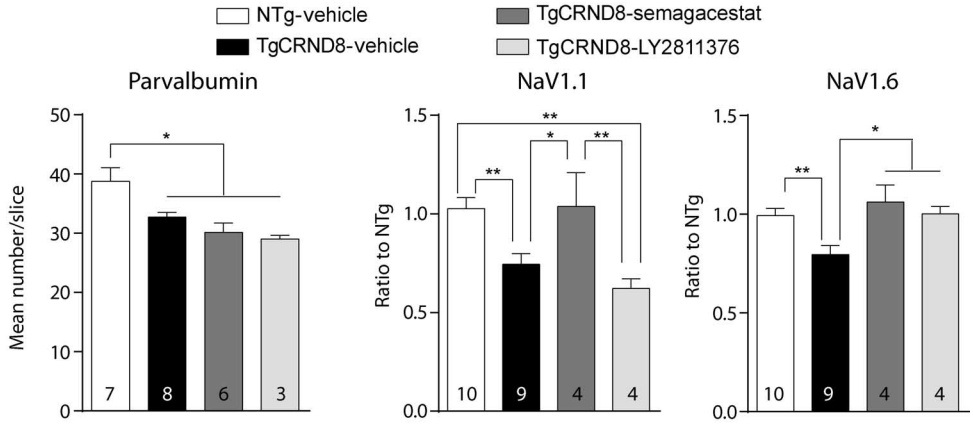

Fig. 6. Differential effect of β-secretase (LY2811376) and γ-secretase (semagacestat) inhibition on PV network. β- and γ-secretase inhibitors did not rescue PV number in the CA1 area of the dorsal hippocampus. However, they both rescued NaV levels albeit using different mechanisms. Whereas semagacestat rescue both NaV1.1 and NaV1.6 levels, LY2811376 only rescued NaV1.6 levels. *, difference between groups (* $P < 0.05$, ** $P < 0.01$).

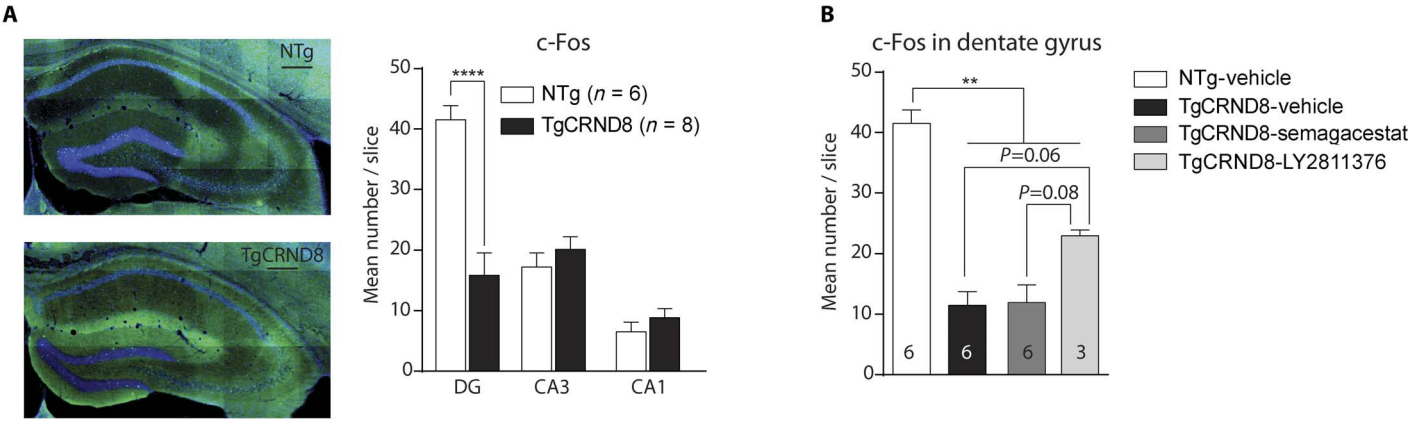

Fig. 7. Differential effect of β-secretase (LY2811376) and γ-secretase (semagacestat) inhibition on dorsal hippocampal activation during the object-place association task. (**A**) Photomicrograph of the dorsal hippocampus from NTg and pre-plaque TgCRND8 mice (c-Fos, green; DAPI, blue). Scale bars, 200 μm. Note the high number in c-Fos–labeled neurons in the dentate gyrus of NTg animals following the object-place association task. This dentate activation is absent in pre-plaque TgCRND8 mice. (**B**) LY2811376, but not semagacestat treatment, increased the number of activated cells in the dentate network during the task, albeit not to the level of NTg animals. *, difference between groups (**$P < 0.01$, ***$P < 0.001$).

hippocampal subregion: $F_{2,24} = 31.22$, $P < 0.0001$; Bonferroni post hoc test: $t_{36} = 8.071$, $P < 0.0001$; Fig. 7A). Therefore, we hypothesized that LY2811376 might rescue normal activation of dentate networks during the object-place association task. Thus, we counted c-Fos–immunolabeled cells in the dentate gyrus of TgCRND8 mice following LY2811376 and semagacestat treatment. We found that treatment with LY2811376, but not semagacestat, increases the number of activated cells in the dentate network during the task, albeit not to the level of NTg animals (one-way ANOVA: $F_{3,17} = 36.53$, $P < 0.001$; Fig. 7B). Therefore, LY2811376 might rescue memory deficits in the object-place association task via an effect on dentate networks.

DISCUSSION

This study demonstrates that pre-plaque TgCRND8 mice exhibit early behavioral alterations only in a subset of hippocampal-dependent tasks associated with drastic deficits in hippocampal inhibitory networks and altered γ oscillations. Strikingly, we showed that different APP metabolites were likely responsible for specific memory deficits in two different tasks. Overall, our study supports the current hypothesis that Aβ is unable to account for all aspects of cognitive impairments in AD, highlighting the complexity of the amyloid pathology.

As the field inches toward early detection of AD to provide precocious treatment (*34*), it is critical to assess the respective role of each APP fragment in the earliest stage of the disease. Hence, we focused our work on young adult TgCRND8 mice, a well-characterized mouse model of AD-like amyloid pathology (*22*). In this mouse model, robust expression of Aβ begins around 10 weeks of age, and amyloid deposits appear at 3 months (*22*). Therefore, we characterized the expression of APP and its proteolytic products in TgCRND8 mice before the "transition point" of high Aβ production (10 weeks of age). By combining Western blot and ELISA dosage approaches, we showed that 1- and 2-month-old TgCRND8 mice expressed low Aβ levels together with high expression of β-CTF in the hippocampus. To determine whether the amyloidogenic state described above (low Aβ and high β-CTF levels) could be linked to alterations in hippocampal functioning as already described in vitro (*9*), we performed in vivo multisite electrophysiological recordings in urethane-anesthetized animals. We found that 2-month-old TgCRND8 mice presented drastic alterations in γ oscillations in the CA1 area. At the cellular level, hippocampal GABAergic neurons are susceptible to Aβ toxicity in vitro and are affected in TgCRND8 mice (*35*). Two interneuron subtypes are considered to be critical in the modulation of hippocampal oscillatory activity: interneurons expressing PV (*24*, *36*) and those expressing SOM (*36*, *37*). We showed that TgCRND8 mice exhibit a marked decrease in the number of PV^+ interneurons, specifically within the CA1 area of the dorsal hippocampus. In addition, the concomitant decreases in the expression of the voltage-gated sodium channel subunits (NaV1.1 and NaV1.6) likely indicate a loss of PV interneurons per se rather than a decrease in PV expression. However, SOM interneurons are preserved in all subfields of the dorsal hippocampus in TgCRND8 mice. These results seem to contradict those reported by Albuquerque *et al.* (*38*), who showed no decrease in the number of PV interneurons but a reduction in the SOM interneurons in 6-month-old TgCRND8 mice. However, in this study, the authors counted PV and SOM cells in the whole hippocampus, including its ventral part, while we focus our investigation on different subfields of the dorsal hippocampal network. Therefore, it is highly possible that interneuron networks might be differentially affected by the amyloid pathology in the dorsal and ventral hippocampus. Nevertheless, our study clearly indicates that pre-plaque young TgCRND8 mice present drastic and specific deficits in dorsal CA1 inhibitory networks associated with altered γ oscillations.

To determine whether these early hippocampal alterations could be linked to cognitive deficits, we performed a large battery of behavioral tasks taxing different types of memories for objects and/or their spatial relationship (novel object recognition, spatial object location, and object-place association tasks), as well as spatial navigation memory (Barnes maze task). These types of memory are known to depend critically on intact hippocampal function, with the notable exception of short-term object recognition memory, which appears to rely more on perirhinal cortex integrity (*21*). We were able to show that 2-month-old TgCRND8 mice present a specific pattern of memory deficits because they were impaired in the spatial object location and the object-place association tasks, while their capacity to discriminate novelty in

the novel object recognition task and their spatial navigation abilities in the Barnes maze task were preserved. The pattern of deficits described in the present study is in partial agreement with those already published in earlier studies on TgCRND8 mice. Although we also found no impairment in spatial navigation memory before increased production of Aβ (*39*, *40*), Francis *et al.* (*39*) reported alterations in the novel object recognition task in 2-month-old TgCRND8 mice. However, this study used both males and females, whereas we only used male mice to avoid the well-known, gender-related variations in amyloid physiopathology (*41*–*43*). In addition, and given the accelerated amyloid pathology in this mouse model, we were extremely careful to control the age of the animals at testing, with less than 1-day variation between all groups (see Materials and Methods). Together, our results indicate that pre-plaque TgCRND8 mice exhibit early deficits only in a limited set of memory tasks, which depends on the dorsal hippocampal region. Further, our results show that specific CA1 subcircuits might be specifically implicated in different processes. As an example, a selective removal of PV interneurons from the CA1 area of the hippocampus induced selective alterations in spatial working memory but not spatial reference memory tasks (*44*).

We also show that both semagacestat and LY2811376 treatments inhibiting Aβ production rescued spatial object location memory, but only the LY2811376 treatment inhibiting β-secretase activity was able to rescue object-place association memory. This result suggests a differential involvement of APP metabolites in memory deficits of 2-month-old TgCRND8 mice. First, the effectiveness of β- and γ-secretase inhibition in reducing both hippocampal Aβ and deficits in the spatial object location task, despite an increased hippocampal β-CTF level after γ-secretase inhibition, suggests that object location memory deficits of 2-month-old TgCRND8 mice are essentially Aβ-dependent. Although these treatments further reduce an already very low level of hippocampal Aβ, it has been shown that very low amounts of intracellular Aβ are sufficient to affect basal synaptic transmission in the CA1 area (*45*). As previously reported, specific alterations in PV networks (*46*, *47*) impair object location memories. Thus, a specific dysfunction of the dorsal CA1 reflected by the reported specific loss of PV interneurons and concomitant alterations in γ oscillatory activities could explain on its own the deficit in the spatial object location task in 2-month-old TgCRND8 male mice. Therefore, we expected that β- and γ-secretase inhibition might rescue PV interneuronal deficits of young TgCRND8 mice. Our results showed that the beneficial effect of both treatments on the spatial object location task might be mediated, in part, by a rescue of the NaV levels, thereby likely restoring normal PV function (*26*). On the other hand, deficits in the object-place association task were more likely related to high levels in hippocampal β-CTF of 2-month-old TgCRND8 mice. β-Secretase inhibition markedly reduced β-CTF and rescued this deficit, whereas the ineffective γ-secretase inhibitor treatment further increased hippocampal β-CTF levels. Alternatively, β-secretase inhibition also increases the α-secretase pathway, leading to increased production of the secreted human APPα, a fragment known to improve memory performance at very low doses on a wide range of tasks and in models of AD (*48*–*50*). Further, the β-secretase cleavage leads to a second important fragment that consists of a large secreted ectodomain (often named sAPPβ). The physiological roles of sAPPβ are poorly known, but there is a general agreement that it has neuroprotective, neurotrophic, and activity-regulating effects similar to sAPPα, although to a lesser extent [see the study of Chasseigneaux and Allinquant (*51*) for a review]. Therefore, it is more likely that memory defects modulated specifically by the β-secretase cleavage are related to the alternative β-CTF fragment clearly identified as neurotoxic (*9*–*11*). Some studies have shown that high levels of β-CTF may have deleterious effects on memory processing (*12*, *15*, *52*). It is unlikely that β-CTF–induced memory deficits in the object-place association task were related to the reported alterations in CA1 PV inhibitory network because semagacestat treatment efficiently rescued the latter but not object-place performances. This task is known to depend on the hippocampal network's integrity (*53*, *54*); thus, other hippocampal subfields might be implicated. To test this hypothesis, we performed c-Fos labeling of activated cells during the object-place association task. We found that the dentate gyrus was the most activated hippocampal area during the task in NTg animals. Further, this dentate activation was markedly reduced in TgCRND8 mice. Therefore, alterations in the object-place association task in young TgCRND8 mice might be due, in part, to alterations in dentate networks. We therefore hypothesized that β-secretase inhibition might rescue normal activation of dentate networks during the object-place association task. LY2811376, but not semagacestat, treatment increased the number of activated cells in the dentate network during the task, albeit not up to the level of NTg. Therefore, β-CTF might preferentially impact dentate network's function. Alternatively, the object-place association task has also been shown to depend on the integrity of the lateral entorhinal cortex (*33*, *55*), one of the main input to the dentate gyrus. Therefore, β-CTF might also precociously affect functioning of brain areas upstream of the hippocampus.

In conclusion, our study clearly indicates that some early memory deficits in a pre-plaque mouse model of AD are Aβ-independent. Most pharmaceutical companies seeking disease-modifying treatments for AD have investigated Aβ-centric therapeutics. However, several of these drugs have met end points in phase 2 and phase 3 trials, because they paradoxically worsened or failed to substantially improve cognitive functions (*6*, *56*). The lack of beneficial effects on cognition suggests that Aβ alone is unable to account for all aspects of the disease (*7*, *8*). Therefore, our study complements the current amyloid hypothesis, which posits that Aβ triggers synaptic and memory dysfunctions in AD (*57*). Our pharmacological results confirm a key role for soluble Aβ peptides in some of the memory deficits described here. In general, our results indicate that selective β-secretase inhibitors remain an attractive approach for AD treatment. However, because β-secretase also interacts with many substrates (*58*), our results would rather favor the use of low-dose multitherapies targeting both β- and γ-secretase for early symptomatic treatment of AD.

MATERIALS AND METHODS

Animals

One- and 2-month-old male TgCRND8 mice and their age-matched NTg littermates were used in this study (1 month old: $n = 5$ NTg and $n = 10$ TgCRND8 mice; mean age, 29.75 ± 0.2 and 30.63 ± 0.23 days, respectively; 2 month old: $n = 92$ NTg and $n = 85$ TgCRND8 mice; mean age, 60.44 ± 0.21 and 60.01 ± 0.18 days, respectively). TgCRND8 mice express a double-mutant (Swedish, KM670/671NL; Indiana, V717F) form of the human APP gene under control of the Syrian hamster PrP gene promoter (*22*). These mice were bred on a hybrid C57BL/6-C3H background and maintained in a temperature- and humidity-controlled room under a 12-hour light/dark cycle (lights on at 7:00 a.m.) with ad libitum access to food and water. Young mice were separated from the mother and housed in groups of two or three at 4 weeks of age and then individually housed 1 week before the start of the experiments, which were conducted during the light phase of

the cycle. Mice homozygote for the retinal degeneration Pdebrd1 (rd) mutation were excluded from the study. In accordance with the European Union laws for animal studies, all procedures were approved by the institutional ethics committee (authorization numbers AL/02/08/04/12 and APAFIS#618-2015050510019910).

ELISA and Western blot

Mice were sacrificed by cervical dislocation, and their brains were carefully dissected on ice. Hippocampi were quickly removed and frozen in liquid nitrogen and stored at −80°C. For quantification of APP, β-CTF, and Aβ, hippocampi were homogenized in 10 volumes of ice-cold radioimmunoprecipitation assay buffer containing protease inhibitor cocktail (Sigma-Aldrich), phosphatase inhibitor cocktail (PhosStop, Roche Life Science), and 1 mM phenylmethylsulfonyl fluoride (Sigma-Aldrich). After centrifugation at 20,000*g* for 20 min at 4°C, supernatants were aliquoted for immunoblot analysis and ELISA. Protein concentration was measured using the Bio-Rad Protein Assay (Bio-Rad).

For immunoblot analysis, samples (20 μg of protein per lane) were separated by 4 to 20% precast gel (Mini-Protean and Criterion TGX precast gels, Bio-Rad) electrophoresis and transferred to nitrocellulose membranes using the Trans-Blot Turbo System (Bio-Rad). After blocking in 5% skimmed milk for 1 hour at room temperature, membranes were incubated overnight at 4°C with primary antibodies diluted in 2% bovine serum albumin (Sigma) in tris-bufferd saline 0.05% Tween 20 (Sigma-Aldrich) followed by anti-mouse or anti-rabbit immunoglobulins conjugated to horseradish peroxidase (Jackson Immunoresearch) for development with enhanced ECL chemiluminescence detection kit (Thermo Fisher Scientific) and exposed to CL-XPosure Film (Thermo Fisher Scientific). After detection, all membranes were reprobed with anti-actin antibody for normalization of total protein. The quantification of the band intensity was performed by densitometry analysis using the ImageJ program.

The different antibodies used were mouse monoclonal anti–Aβ (6E10, 1:10,000; Covance), rabbit polyclonal anti-APP, C terminus (1:4000; Sigma-Aldrich), mouse monoclonal anti-actin (1:10,000; Sigma-Aldrich), rabbit polyclonal anti-NaV1.1 and rabbit polyconal anti-NaV1.6 (1:500 and 1:1000, respectively; Alomone Labs), and peroxidase-conjugated AffiniPure goat anti-mouse and goat anti-rabbit (1:10,000; Jackson Immunoresearch). For sandwich ELISA, we used the human Aβ(1–42) high sensitivity ELISA kits (IBL International). All ELISA assays were performed according to the manufacturer's protocol. The signal was normalized to the protein concentration for each sample. All dosages were done using duplicates, and samples with variation >10% between duplicates were discarded from analysis.

In vivo electrophysiology under urethane anesthesia

Mice under urethane (1.8 g/kg; Sigma-Aldrich) terminal anesthesia were placed in a stereotaxic apparatus after the complete loss of tail and paw-pinch retraction reflexes. Recording coordinates in the dorsal hippocampus were calculated from bregma (dorsal hippocampus: anteroposterior, −2 mm; mediolateral, ±0.15 mm). Recordings were done with a linear 16-channel silicon probe (NeuroNexus, A1x16-2mm-50-177) connected to an AlphaLab recording system (Alpha Omega). Raw signal was amplified (200×), filtered between 0 and 9 kHz, and digitalized at 22 kHz. Silicon probes were painted with 2% DiI solution (Sigma-Aldrich) for localization. Analyses were carried out using custom-made scripts in Matlab (MathWorks). When present, slow drift and electrical noise were removed using the Chronux signal processing toolbox (*59*). Local field potential data were downsampled to 2200 Hz and filtered between 0.1 and 500 Hz. Spectral analysis was carried with the Chronux toolbox with a time-frequency product of three and five tapers. Time-frequency analyses were done on a 4-s window moved across the data in 1-s increments. Urethane anesthesia was characterized by alternating θ and non-θ states (*60*). Only periods associated with θ (θ/δ power ratio > 5) were analyzed. Spectral power was calculated as the integrated power for θ (3 to 9 Hz under urethane anesthesia), SG (25 to 45 Hz), and FG (60 to 100 Hz).

Behavior

Novel object recognition, spatial object location, and object-place association tasks.

The recognition memory tasks used in this study were based on the spontaneous tendency of mice to preferentially explore a new object (novel object recognition task), an object that moved to a new location (spatial object location task), or a known object replacing a different object (object-place association task). These tasks were performed in a square plexiglas open field (52 cm × 52 cm) with black walls (40 cm high) and a white floor divided into 25 equal squares by black lines. A striped card was fixed against a wall. The device was illuminated by an indirect halogen light (open field center, 40 lux), and a radio played a background noise 2 m from the device (open field center, 45 ± 5 dB). Nine different objects were used (two for the habituation phases, two for the novel object recognition task, three for the spatial object location task, and two for the object-place task), which differed in size (10 to 20 cm), material (metal, glass, or plastic), shape, and color. Each object was available in duplicate or triplicate (one set for each trial). Between each trial, the walls, floor, and objects were wiped with 70% ethanol. Object exploration time was recorded and defined as the nose pointing toward the object within 1 cm. Before testing, all mice received a habituation trial of 10 min with an object placed in the center of the open field, returned to their home cage for 3 hours, and then received another 10-min habituation trial with a new object.

For the novel object recognition task, mice explored the configuration of two identical objects during a 10-min acquisition trial, returned to their home cage for 3 hours, and then received a 10-min retention trial, during which one of the familiar objects was replaced by an unfamiliar new one. A memory index was calculated and defined as: (time spent exploring the new object − time spent exploring the old object)/total exploration time for the two objects during the 10-min retention trial.

For the spatial object location task, mice first explored the configuration of three objects placed in three corners of the open field (each approximately 10 cm from walls) during a 10-min acquisition trial, returned to their home cage for 3 hours, and then received a 10-min retention trial with a new spatial configuration resulting from the shift of an object from one corner to the opposite free corner of the open field. A memory index was calculated and defined as: (time spent exploring the displaced object – average exploration time of nondisplaced objects)/total exploration time for the three objects during the 10-min retention trial.

For the object-place association task, mice explored the configuration of two different objects during a 10-min acquisition trial, returned to their home cage for 3 hours, and then received a 10-min retention trial, during which the two initial objects were replaced by two copies of one of these objects. Thus, apparently one known object remained unchanged, while its copy took the place of the different object. A memory index was calculated and defined as: (time spent

exploring the replacing object − time spent exploring the unchanged object)/total exploration time for the two objects during the 10-min retention trial.

Barnes maze.

The Barnes maze task (*31*) is particularly relevant for assessing spatial navigation memory in mice because of their natural ability to find an escape through small holes and their physiological adaptation to the dry-land maze compared to their poor adaptation to tasks based on water escape responses, such as in the Morris water maze (*61*). After a 3-day habituation to the tube leading to the home cage of the mouse, mice were trained for 5 days (three daily trials, 180-s cutoff, intertrial interval of 15 min) to find the target hole among 12 identical holes (diameter, 4 cm) equally distributed (space between holes, 15 cm) at 9 cm from the edge of a 1-cm-diameter circular board. During this acquisition phase, the target hole was connected to the tube leading to the home cage. The target hole was at a fixed location in the testing room, which provided various extra-maze, auditory, olfactory, and visual cues, such as the rack holding the cages of the other mice, a background noise from a radio, which played 2 m from the center of the platform (maze center, 45 ± 5 dB), furniture, pictures, and an overhead lighting (800 lux at the maze center). An opaque polyvinyl chloride starting cylinder, placed in the center of the maze, was used to confine the mice at the center of the platform before being lifted at the start of each trial. Between trials, the maze and holes were wiped with 70% ethanol and pseudorandomly rotated to minimize odor-based strategies. For each trial, we evaluated the latency of the first visit to the target hole (nose poke in the target hole). After the 5 days of acquisition, mice were subjected to a probe test (120 s) with all the holes closed. Preferential exploration of the target hole (calculated as the ratio between the number of visits to the target hole and the total number of hole visits) was considered to reflect good spatial navigation memory.

Pharmacology

To target APP metabolites and their behavioral impacts, mice were treated by oral gavage with either the vehicle alone (hydroxypropyl cellulose; Sigma-Aldrich), a β-secretase inhibitor (LY-2811376; MedChem Express; 15 mg/kg every 2 days between 1 and 2 months of age), or a γ-secretase inhibitor (semagacestat; AbMole; 10 mg/kg per day for 6 days). The doses of the secretases were selected according to the studies of May *et al.* (*32*) and Mitani *et al.* (*12*), respectively. On the last 2 days of treatment, animals were first tested in the spatial object location task and then in the object-place association task. Three hours after the last injection, a subset of treated mice were sacrificed with an overdose of sodium pentobarbital (200 mg/kg intraperitoneally) and decapitated. Bilateral hippocampi were rapidly microdissected, frozen in liquid nitrogen, and stored at −80°C before ELISA and Western blot quantifications.

Histological study

Perfusion and tissue preparation.

Mice were sacrificed with an overdose of sodium pentobarbital (200 mg/kg intraperitoneally) and transcardially perfused in 0.1% heparin phosphate-buffered saline (PBS) and 4% paraformaldehyde [PFA; in phosphate buffer (PB) pH 7.4; 4°C]. Brains were tidily removed, postfixed in a 4% PFA solution for 24 hours, and cryoprotected in a saccharose solution (20% in PB, 0.1 M; pH 7.4; 4°C) for 48 hours before being frozen with isopentane (−40°C) and subsequently stored at −80°C. Thin (20 μm) frontal brain sections from the dorsal hippocampus (bregma, −1.34 to 2.06 mm) were cut with a cryostat and mounted on gelatin slides.

Immunohistochemistry.

Sections were pretreated in 1% H_2O_2 (15 min) and in sodium citrate (10 mM; pH 8; 30 min at 80°C). Sections were then rinsed in 0.1 M PBS (3 × 10 min) before being blocked in 5% donkey serum (1 hour), followed by incubation with primary antibodies in 2% donkey serum and 0.1% Triton X-100 (24 hours at 4°C). We used mouse monoclonal PV (Sigma; 1:4000), rabbit polyclonal SOM (Santa Cruz; 1:500), and rabbit polyclonal c-Fos (Santa Cruz; 1:500) primary antibodies. The next day, sections were rinsed three times in 0.1 M PBS (3 × 10 min) before a 2-hour incubation in the dark with secondary antibodies (anti-rabbit Alexa 488, 1:1000; antimouse Alexa 568, 1:1000; Invitrogen Molecular Probes). Last, sections were rinsed three times in 0.1 M PBS (3 × 10 min) and rapidly in ultrapure water before being mounted with DAPI fluoromount (Southern Biotech). Cell quantification was done as described in the study of Ducharme *et al.* (*62*). Briefly, one section every 120 μm was analyzed, which means that four to six sections were evaluated per animal. This set of sections encompassed the dorsal portion of the hippocampus. Photomicrographs were captured using a fluorescence microscope coupled to an ApoTome module (Zeiss), and all labeled cells were counted bilaterally by an experimenter blinded to the genotype. The cells were identified on the basis of shape and size (roughly 10 to 20 μm in diameter), and cells with a large range of staining intensity were included. The counts were performed for each hippocampal subfield individually using the ImageJ software.

Statistical analyses

Analyses were done with GraphPad 6 (Prism). Data are expressed as means ± SEM. Memory index was compared to the 0 chance level (no detection of the new object or spatial change) with a one-sample Student's *t* test. Unpaired *t* tests were used to compare genotypes. All the other analyses were done using a two-way ANOVA (with or without repeated measures) except for the exploration time analysis with pharmacological treatment, where three-way ANOVA was used (Matlab). Because NTg- and TgCRND8-vehicle mice do not differ from nontreated animals, they were sometimes pooled together to decrease the number of animals used in the study. In case of significant ANOVA, multiple comparisons among groups were performed using Bonferroni's multiple-comparisons test. The threshold for statistical significance was set at $P < 0.05$. The experimenter was blinded to the treatment groups until the end of behavioral testing.

SUPPLEMENTARY MATERIALS

Supplementary material for this article is available at http://advances.sciencemag.org/cgi/content/full/3/2/e1601068/DC1

fig. S1. Western blot using the 6E10 antibody and quantification of the levels of two forms of the human APP: the full-length hAPP and the β-CTF.
fig. S2. Total exploration time during the spatial object location task.
fig. S3. Total exploration time during the object-place association task.
fig. S4. Relative visits to the target during the probe test of the Barnes maze task.
fig. S5. Total exploration time during the novel object recognition task.
fig. S6. Memory index in NTg animals following pharmacological treatment.
fig. S7. Total exploration time during the spatial object location task with pharmacological treatment.
fig. S8. Total exploration time during the object-place task with pharmacological treatment.

REFERENCES AND NOTES

1. D. J. Selkoe, Toward a comprehensive theory for Alzheimer's disease. Hypothesis: Alzheimer's disease is caused by the cerebral accumulation and cytotoxicity of amyloid β-protein. *Ann. N. Y. Acad. Sci.* **924**, 17–25 (2000).
2. J. J. Palop, L. Mucke, Amyloid-β–induced neuronal dysfunction in Alzheimer's disease: From synapses toward neural networks. *Nat. Neurosci.* **13**, 812–818 (2010).

3. C. Haass, D. J. Selkoe, Soluble protein oligomers in neurodegeneration: Lessons from the Alzheimer's amyloid β-peptide. *Nat. Rev. Mol. Cell Biol.* **8**, 101–112 (2007).
4. L. Mucke, E. Masliah, G.-Q. Yu, M. Mallory, E. M. Rockenstein, G. Tatsuno, K. Hu, D. Kholodenko, K. Johnson-Wood, L. McConlogue, High-level neuronal expression of $a\beta_{1-42}$ in wild-type human amyloid protein precursor transgenic mice: Synaptotoxicity without plaque formation. *J. Neurosci.* **20**, 4050–4058 (2000).
5. D. J. Selkoe, The molecular pathology of Alzheimer's disease. *Neuron* **6**, 487–498 (1991).
6. J. A. Mikulca, V. Nguyen, D. A. Gajdosik, S. G. Teklu, E. A. Giunta, E. A. Lessa, C. H. Tran, E. C. Terak, R. B. Raffa, Potential novel targets for Alzheimer pharmacotherapy: II. Update on secretase inhibitors and related approaches. *J. Clin. Pharm. Ther.* **39**, 25–37 (2014).
7. S. W. Pimplikar, Reassessing the amyloid cascade hypothesis of Alzheimer's disease. *Int. J. Biochem. Cell Biol.* **41**, 1261–1268 (2009).
8. T. E. Golde, L. S. Schneider, E. H. Koo, Anti-aβ therapeutics in Alzheimer's disease: The need for a paradigm shift. *Neuron* **69**, 203–213 (2011).
9. R. Goutagny, N. Gu, C. Cavanagh, J. Jackson, J.-G. Chabot, R. Quirion, S. Krantic, S. Williams, Alterations in hippocampal network oscillations and theta-gamma coupling arise before Aβ overproduction in a mouse model of Alzheimer's disease. *Eur. J. Neurosci.* **37**, 1896–1902 (2013).
10. I. Lauritzen, R. Pardossi-Piquard, C. Bauer, E. Brigham, J.-D. Abraham, S. Ranaldi, P. Fraser, P. St-George-Hyslop, O. Le Thuc, V. Espin, L. Chami, J. Dunys, F. Checler, The β-secretase-derived C-terminal fragment of βAPP, C99, but not Aβ, is a key contributor to early intraneuronal lesions in triple-transgenic mouse hippocampus. *J. Neurosci.* **32**, 16243–16255 (2012).
11. K.-A. Chang, Y.-H. Suh, Pathophysiological roles of amyloidogenic carboxy-terminal fragments of the β-amyloid precursor protein in Alzheimer's disease. *J. Pharmacol. Sci.* **97**, 461–471 (2005).
12. Y. Mitani, J. Yarimizu, K. Saita, H. Uchino, H. Akashiba, Y. Shitaka, K. Ni, N. Matsuoka, Differential effects between γ-secretase inhibitors and modulators on cognitive function in amyloid precursor protein-transgenic and nontransgenic mice. *J. Neurosci.* **32**, 2037–2050 (2012).
13. R. L. Neve, F. M. Boyce, D. L. McPhie, J. Greenan, M. L. Oster-Granite, Transgenic mice expressing APP-C100 in the brain. *Neurobiol. Aging* **17**, 191–203 (1996).
14. R. Tamayev, L. D'Adamio, Inhibition of γ-secretase worsens memory deficits in a genetically congruous mouse model of Danish dementia. *Mol. Neurodegener.* **7**, 19 (2012).
15. R. Tamayev, S. Matsuda, O. Arancio, L. D'Adamio, β- but not γ-secretase proteolysis of APP causes synaptic and memory deficits in a mouse model of dementia. *EMBO Mol. Med.* **4**, 171–179 (2012).
16. D. L. Vogt, sD. Thomas, V. Galvan, D. E. Bredesen, B. T. Lamb, S. W. Pimplikar, Abnormal neuronal networks and seizure susceptibility in mice overexpressing the APP intracellular domain. *Neurobiol. Aging* **32**, 1725–1729 (2011).
17. M. Willem, S. Tahirovic, M. A. Busche, S. V. Ovsepian, M. Chafai, S. Kootar, D. Hornburg, L. D. B. Evans, S. Moore, A. Daria, H. Hampel, V. Müller, C. Giudici, B. Nuscher, A. Wenninger-Weinzierl, E. Kremmer, M. T. Heneka, D. R. Thal, V. Giedraitis, L. Lannfelt, U. Müller, F. J. Livesey, F. Meissner, J. Herms, A. Konnerth, H. Marie, C. Haass, η-Secretase processing of APP inhibits neuronal activity in the hippocampus. *Nature* **526**, 443–447 (2015).
18. M. Didic, E. J. Barbeau, O. Felician, E. Tramoni, E. Guedj, M. Poncet, M. Ceccaldi, Which memory system is impaired first in Alzheimer's disease? *J. Alzheimers Dis.* **27**, 11–22 (2011).
19. K. Vlček, Spatial navigation impairment in healthy aging and Alzheimer's disease, in *The Clinical Spectrum of Alzheimer's Disease–The Charge Toward Comprehensive Diagnostic and Therapeutic Strategies*, S. De La Monte, Ed. (InTech, ed. 5, 2011).
20. J. Hort, J. Laczó, M. Vyhnálek, M. Bojar, J. Bureš, K. Vlček, Spatial navigation deficit in amnestic mild cognitive impairment. *Proc. Natl. Acad. Sci. U.S.A.* **104**, 4042–4047 (2007).
21. K. E. Ameen-Ali, A. Easton, M. J. Eacott, Moving beyond standard procedures to assess spontaneous recognition memory. *Neurosci. Biobehav. Rev.* **53**, 37–51 (2015).
22. M. A. Chishti, D.-S. Yang, C. Janus, A. L. Phinney, P. Horne, J. Pearson, R. Strome, N. Zuker, J. Loukides, J. French, S. Turner, G. Lozza, M. Grilli, S. Kunicki, C. Morissette, J. Paquette, F. Gervais, C. Bergeron, P. E. Fraser, G. A. Carlson, P. St. George-Hyslop, D. Westaway, Early-onset amyloid deposition and cognitive deficits in transgenic mice expressing a double mutant form of amyloid precursor protein 695. *J. Biol. Chem.* **276**, 21562–21570 (2001).
23. C. Cavanagh, J. Colby-Milley, D. Bouvier, M. Farso, J.-G. Chabot, R. Quirion, S. Krantic, βCTF-correlated burst of hippocampal TNFα occurs at a very early, pre-plaque stage in the TgCRND8 mouse model of Alzheimer's disease. *J. Alzheimers Dis.* **36**, 233–238 (2013).
24. V. S. Sohal, F. Zhang, O. Yizhar, K. Deisseroth, Parvalbumin neurons and gamma rhythms enhance cortical circuit performance. *Nature* **459**, 698–702 (2009).
25. T. Dugladze, I. Vida, A. B. Tort, A. Gross, J. Otahal, U. Heinemann, N. J. Kopell, T. Gloveli, Impaired hippocampal rhythmogenesis in a mouse model of mesial temporal lobe epilepsy. *Proc. Natl. Acad. Sci. U.S.A.* **104**, 17530–17535 (2007).
26. L. Verret, E. O. Mann, G. B. Hang, A. M. I. Barth, I. Cobos, K. Ho, N. Devidze, E. Masliah, A. C. Kreitzer, I. Mody, L. Mucke, J. J. Palop, Inhibitory interneuron deficit links altered network activity and cognitive dysfunction in Alzheimer model. *Cell* **149**, 708–721 (2012).
27. L. C. Schmid, M. Mittag, S. Poll, J. Steffen, J. Wagner, H.-R. Geis, I. Schwarz, B. Schmidt, M. K. Schwarz, S. Remy, M. Fuhrmann, Dysfunction of somatostatin-positive interneurons associated with memory deficits in an Alzheimer's disease model. *Neuron* **92**, 114–125 (2016).
28. S. N. Burke, A. P. Maurer, S. Nematollahi, A. R. Uprety, J. L. Wallace, C. A. Barnes, The influence of objects on place field expression and size in distal hippocampal CA1. *Hippocampus* **21**, 783–801 (2011).
29. F. L. Assini, M. Duzzioni, R. N. Takahashi, Object location memory in mice: Pharmacological validation and further evidence of hippocampal CA1 participation. *Behav. Brain Res.* **204**, 206–211 (2009).
30. N. J. Goodrich-Hunsaker, M. R. Hunsaker, R. P. Kesner, The interactions and dissociations of the dorsal hippocampus subregions: How the dentate gyrus, CA3, and CA1 process spatial information. *Behav. Neurosci.* **122**, 16–26 (2008).
31. C. A. Barnes, Memory deficits associated with senescence: A neurophysiological and behavioral study in the rat. *J. Comp. Physiol. Psychol.* **93**, 74–104 (1979).
32. P. C. May, R. A. Dean, S. L. Lowe, F. Martenyi, S. M. Sheehan, L. N. Boggs, S. A. Monk, B. M. Mathes, D. J. Mergott, B. M. Watson, S. L. Stout, D. E. Timm, E. Smith Labell, C. R. Gonzales, M. Nakano, S. S. Jhee, M. Yen, L. Ereshefsky, T. D. Lindstrom, D. O. Calligaro, P. J. Cocke, D. Greg Hall, S. Friedrich, M. Citron, J. E. Audia, Robust central reduction of amyloid-β in humans with an orally available, non-peptidic β-secretase inhibitor. *J. Neurosci.* **31**, 16507–16516 (2011).
33. D. I. G. Wilson, S. Watanabe, H. Milner, J. A. Ainge, Lateral entorhinal cortex is necessary for associative but not nonassociative recognition memory. *Hippocampus* **23**, 1280–1290 (2013).
34. A. Nordberg, Dementia in 2014: Towards early diagnosis in Alzheimer disease. *Nat. Rev. Neurol.* **11**, 69–70 (2015).
35. S. Krantic, N. Isorce, N. Mechawar, M. A. Davoli, E. Vignault, M. Albuquerque, J.-G. Chabot, E. Moyse, J.-P. Chauvin, I. Aubert, J. McLaurin, R. Quirion, Hippocampal GABAergic neurons are susceptible to amyloid-β toxicity in vitro and are decreased in number in the Alzheimer's disease TgCRND8 mouse model. *J. Alzheimers Dis.* **29**, 293–308 (2012).
36. D. Lapray, B. Lasztoczi, M. Lagler, T. J. Viney, L. Katona, O. Valenti, K. Hartwich, Z. Borhegyi, P. Somogyi, T. Klausberger, Behavior-dependent specialization of identified hippocampal interneurons. *Nat. Neurosci.* **15**, 1265–1271 (2012).
37. C. Varga, P. Golshani, I. Soltesz, Frequency-invariant temporal ordering of interneuronal discharges during hippocampal oscillations in awake mice. *Proc. Natl. Acad. Sci. U.S.A.* **109**, E2726–E2734 (2012).
38. M. S. Albuquerque, I. Mahar, M. A. Davoli, J.-G. Chabot, N. Mechawar, R. Quirion, S. Krantic, Regional and sub-regional differences in hippocampal GABAergic neuronal vulnerability in the TgCRND8 mouse model of Alzheimer's disease. *Front. Aging Neurosci.* **7**, 30 (2015).
39. B. M. Francis, J. Kim, M. E. Barakat, S. Fraenkl, Y. H. Yücel, S. Peng, B. Michalski, M. Fahnestock, J. McLaurin, H. T. J. Mount, Object recognition memory and BDNF expression are reduced in young TgCRND8 mice. *Neurobiol. Aging* **33**, 555–563 (2012).
40. C. Janus, J. Pearson, J. McLaurin, P. M. Mathews, Y. Jiang, S. D. Schmidt, M. A. Chishti, P. Horne, D. Heslin, J. French, H. T. J. Mount, R. A. Nixon, M. Mercken, C. Bergeron, P. E. Fraser, P. St George-Hyslop, D. Westaway, Aβ peptide immunization reduces behavioural impairment and plaques in a model of Alzheimer's disease. *Nature* **408**, 979–982 (2000).
41. A. Assini, S. Cammarata, A. Vitali, M. Colucci, L. Giliberto, R. Borghi, M. L. Inglese, S. Volpe, S. Ratto, F. Dagna-Bricarelli, C. Baldo, A. Argusti, P. Odetti, A. Piccini, M. Tabaton, Plasma levels of amyloid β-protein 42 are increased in women with mild cognitive impairment. *Neurology* **63**, 828–831 (2004).
42. K. Irvine, K. R. Laws, T. M. Gale, T. K. Kondel, Greater cognitive deterioration in women than men with Alzheimer's disease: A meta analysis. *J. Clin. Exp. Neuropsychol.* **34**, 989–998 (2012).
43. S. A. Shumaker, C. Legault, S. R. Rapp, L. Thal, R. B. Wallace, J. K. Ockene, S. L. Hendrix, B. N. Jones III, A. R. Assaf, R. D. Jackson, J. M. Kotchen, S. Wassertheil-Smoller, J. Wactawski-Wende; WHIMS Investigators, Estrogen plus progestin and the incidence of dementia and mild cognitive impairment in postmenopausal women: The Women's Health Initiative Memory Study: A randomized controlled trial. *JAMA* **289**, 2651–2662 (2003).
44. A. J. Murray, J.-F. Sauer, G. Riedel, C. McClure, L. Ansel, L. Cheyne, M. Bartos, W. Wisden, P. Wulff, Parvalbumin-positive CA1 interneurons are required for spatial working but not for reference memory. *Nat. Neurosci.* **14**, 297–299 (2011).
45. C. Ripoli, S. Cocco, D. D. Li Puma, R. Piacentini, A. Mastrodonato, F. Scala, D. Puzzo, M. D'Ascenzo, C. Grassi, Intracellular accumulation of amyloid-β (Aβ) protein plays a major role in Aβ-induced alterations of glutamatergic synaptic transmission and plasticity. *J. Neurosci.* **34**, 12893–12903 (2014).

46. E. C. Fuchs, A. R. Zivkovic, M. O. Cunningham, S. Middleton, F. E. N. Lebeau, D. M. Bannerman, A. Rozov, M. A. Whittington, R. D. Traub, J. N. P. Rawlins, H. Monyer, Recruitment of parvalbumin-positive interneurons determines hippocampal function and associated behavior. *Neuron* **53**, 591–604 (2007).
47. T. Korotkova, E. C. Fuchs, A. Ponomarenko, J. von Engelhardt, H. Monyer, NMDA receptor ablation on parvalbumin-positive interneurons impairs hippocampal synchrony, spatial representations, and working memory. *Neuron* **68**, 557–569 (2010).
48. H. Meziane, J.-C. Dodart, C. Mathis, S. Little, J. Clemens, S. M. Paul, A. Ungerer, Memory-enhancing effects of secreted forms of the β-amyloid precursor protein in normal and amnestic mice. *Proc. Natl. Acad. Sci. U.S.A.* **95**, 12683–12688 (1998).
49. A. Bour, S. Little, J.-C. Dodart, C. Kelche, C. Mathis, A secreted form of the β-amyloid precursor protein ($sAPP_{695}$) improves spatial recognition memory in OF1 mice. *Neurobiol. Learn. Mem.* **81**, 27–38 (2004).
50. R. Fol, J. Braudeau, S. Ludewig, T. Abel, S. W. Weyer, J.-P. Roederer, F. Brod, M. Audrain, A.-P. Bemelmans, C. J. Buchholz, M. Korte, N. Cartier, U. C. Müller, Viral gene transfer of APPsα rescues synaptic failure in an Alzheimer's disease mouse model. *Acta Neuropathol.* **131**, 247–266 (2016).
51. S. Chasseigneaux, B. Allinquant, Functions of Aβ, sAPPα and sAPPβ: Similarities and differences. *J. Neurochem.* **120** (suppl. 1), 99–108 (2012).
52. F. Biundo, K. Ishiwari, D. Del Prete, L. D'Adamio, Deletion of the γ-secretase subunits Aph1B/C impairs memory and worsens the deficits of knock-in mice modeling the Alzheimer-like familial Danish dementia. *Oncotarget* **7**, 11923–11944 (2016).
53. T. J. Bussey, J. Duck, J. L. Muir, J. P. Aggleton, Distinct patterns of behavioural impairments resulting from fornix transection or neurotoxic lesions of the perirhinal and postrhinal cortices in the rat. *Behav. Brain Res.* **111**, 187–202 (2000).
54. D. G. Mumby, S. Gaskin, M. J. Glenn, T. E. Schramek, H. Lehmann, Hippocampal damage and exploratory preferences in rats: Memory for objects, places, and contexts. *Learn. Mem.* **9**, 49–57 (2002).
55. D. I. G. Wilson, R. F. Langston, M. I. Schlesiger, M. Wagner, S. Watanabe, J. A. Ainge, Lateral entorhinal cortex is critical for novel object-context recognition. *Hippocampus* **23**, 352–366 (2013).
56. E. Karran, J. Hardy, Antiamyloid therapy for Alzheimer's disease—Are we on the right road? *N. Engl. J. Med.* **370**, 377–378 (2014).
57. D. J. Selkoe, J. Hardy, The amyloid hypothesis of Alzheimer's disease at 25 years. *EMBO Mol. Med.* **8**, 595–608 (2016).
58. M. L. Hemming, J. E. Elias, S. P. Gygi, D. J. Selkoe, Identification of β-secretase (BACE1) substrates using quantitative proteomics. *PLOS ONE* **4**, e8477 (2009).
59. H. Bokil, P. Andrews, J. E. Kulkarni, S. Mehta, P. P. Mitra, Chronux: A platform for analyzing neural signals. *J. Neurosci. Methods* **192**, 146–151 (2010).
60. S. Pagliardini, S. Gosgnach, C. T. Dickson, Spontaneous sleep-like brain state alternations and breathing characteristics in urethane anesthetized mice. *PLOS ONE* **8**, e70411 (2013).
61. I. Q. Whishaw, J.-A. Tomie, Of mice and mazes: Similarities between mice and rats on dry land but not water mazes. *Physiol. Behav.* **60**, 1191–1197 (1996).
62. G. Ducharme, G. C. Lowe, R. Goutagny, S. Williams, Early alterations in hippocampal circuitry and theta rhythm generation in a mouse model of prenatal infection: Implications for schizophrenia. *PLOS ONE* **7**, e29754 (2012).

Acknowledgments: We thank O. Bildstein, G. Edomwonyi, and O. Egesi for animal care. **Funding:** This work was supported by a Career Integration Grant from the Marie Curie program of the European Research Council (grant # PCIG10-GA-2011-303573 to R.G.), the Neurex network (grants to R.G. and C.H.), Fondation Fyssen (to R.G.), France Alzheimer Haut-Rhin (to C.M.), the French Ministry of Education and Research (to V.H. and J.-B.B.), the CNRS, and the Université de Strasbourg. **Author contributions:** C.M., J.-B.B., and R.G. conceived the experiments. V.H., C.H., J.-B.B., and K.H. performed the experiments. V.H., C.H., and R.G. analyzed the data. C.S. managed the mouse colony. V.H., C.M., and R.G. wrote the paper. **Competing interests:** The authors declare that they have no competing interests. **Data and materials availability:** All data needed to evaluate the conclusions in the paper are present in the paper and/or the Supplementary Materials. Additional data related to this paper may be requested from the authors.

Submitted 12 May 2016
Accepted 25 January 2017
Published 24 February 2017
10.1126/sciadv.1601068

Citation: V. Hamm, C. Héraud, J.-B. Bott, K. Herbeaux, C. Strittmatter, C. Mathis, R. Goutagny, Differential contribution of APP metabolites to early cognitive deficits in a TgCRND8 mouse model of Alzheimer's disease. *Sci. Adv.* **3**, e1601068 (2017).

Differential contribution of APP metabolites to early cognitive deficits in a TgCRND8 mouse model of Alzheimer's disease

Valentine Hamm, Céline Héraud, Jean-Bastien Bott, Karine Herbeaux, Carole Strittmatter, Chantal Mathis and Romain Goutagny

Sci Adv **3** (2), e1601068.
DOI: 10.1126/sciadv.1601068